Regenerative Therapy 26 (2024) 432–441

Contents lists available at ScienceDirect

Regenerative Therapy

journal homepage: http://www.elsevier.com/locate/reth

Original Article

# Induction of periodontal ligament-derived mesenchymal stromal cell-like cells from human induced pluripotent stem cells

Jiacheng Wang, Kazuki Morita, Takanori Iwata*

*Department of Periodontology, Graduate School of Medical and Dental Sciences, Tokyo Medical and Dental University, 1-5-45 Yushima, Bunkyo-ku, Tokyo 113-8510, Japan*

ARTICLE INFO

*Article history:*
Received 22 February 2024
Received in revised form
9 May 2024
Accepted 14 May 2024

*Keywords:*
Cell differentiation
Cytokine(s)
Extracellular matrix (ECM)
Periodontal ligament (PDL)
Stem cell(s)

ABSTRACT

*Introduction:* Periodontal disease is a common oral infection which affects the tooth-supportive tissues directly. Considering the limitation of present regenerative treatments for severe periodontal cases, cytotherapies have been gradually introduced. Human periodontal ligament-derived mesenchymal stromal cells (hPDLMSCs), while identified as one of the promising cell sources for periodontal regenerative therapy, still hold some problems in the clinical application especially their limited life span. To solve the problems, human induced pluripotent stem cells (hiPSCs) are taken into consideration as a robust supply for hPDLMSCs.

*Methods:* The induction of hPDLMSCs was performed based on the generation of neural crest-like cells (NCLCs) from hiPSCs. Fibronectin and laminin were tested as coating materials for NCLCs differentiation when following previous protocol, and the characteristics of induced cells were identified by flow cytometry and RT-qPCR for evaluating the induction efficiency. Subsequently, selected dental ectoderm signaling-related cytokines were applied for hPDLMSCs induction for 14 days, and dental mesenchyme-related genes, dental follicle-related genes and hPDL-related genes were tested by RT-qPCR for the evaluation of differentiation.

*Results:* Compared to the 58% in laminin-coated condition, fibronectin-coated condition had a higher induction efficiency of $CD271^{high}$ cells as 86% after 8-day induction, while the mesenchymal potential of induced NCLCs was similar between two coating materials.

It was shown that the gene expressions of dental mesenchyme, dental follicles and hPDL cells were significantly enhanced with the stimulation of the combination with fibroblast growth factor 8b (FGF8b), FGF2, and bone morphogenetic protein 4 (BMP4).

*Conclusion:* FN coating was more effective in NCLCs induction, and the FGF8b+FGF2+BMP4 growth factor cocktail was effective in hPDLMSC-like cell generation. These findings underscored the likely regenerative potential of hiPSCs as an applicable and promising curative strategy for periodontal diseases.



*Abbreviations:* hPDLMSCs, human periodontal ligament-derived mesenchymal stromal cells; hiPSCs, human induced pluripotent stem cells; NCCs, neural crest cells; FN, fibronectin; LM, laminin; iNCLCs, induced neural crest-like cells; ECM, extracellular matrix; FGF8, fibroblast growth factor 8; FGF2, fibroblast growth factor 2; BMP4, bone morphogenetic protein 4; EDA, Ectodysplasin A; EGF, epidermal growth factor; EB, embryonic body; ESCs, embryonic stem cells; *ACTB*, actin beta; *NGFR*, nerve growth factor receptor; *SOX10*, SRY-related HMG-box 10; *TFAP2A*, transcription factor activating enhancer binding protein 2 alpha; *FOXD3*, forkhead box D3; *PAX6*, paired box 6; *POU5F1*, POU Class 5 Homeobox 1; *PAX9*, paired box gene 9; *LHX8*, LIM Homeobox 8; *DLX1*, distal-less homeobox 3; *MSX1*, msh homeobox 1; *FOXF1*, forkhead box protein F1; *FOXF2*, forkhead box protein F2; *POSTN*, periostin; *S100A4*, S100 calcium-binding protein A4; BMMSCs, bone marrow mesenchymal stem cells; hGFs, human gingival fibroblast cell; *SPP1*, secreted phosphoprotein 1; *BGLAP*, Bone Gamma-Carboxyglutamate Protein; *LPL*, Lipoprotein Lipase; *PPARγ*, Peroxisome Proliferator Activated Receptor Gamma.

* Corresponding author.
*E-mail address:* iwata.peri@tmd.ac.jp (T. Iwata).

Peer review under responsibility of the Japanese Society for Regenerative Medicine.

https://doi.org/10.1016/j.reth.2024.05.005

## 1. Introduction

Periodontal disease is an inflammatory condition initiated by plaque biofilm that destroys the structures supporting the teeth, ultimately resulting in tooth loss if left untreated [1]. Approximately 19% of adults are affected by this disease worldwide, and their damaged alveolar bone needs appropriate therapeutic methods for reconstruction [2]. Periodontal regenerative therapy, such as guided tissue regeneration and bone grafts, has been developed for decades and applied for this purpose [3]. Although it offered an option for reconstructing the alveolar bone, the clinical application is still limited due to the indications and instability of bone formation [4]. For better curative effects, including the regeneration of periodontal ligament (PDL) that traditional treatments are hard to achieve, cytotherapeutic approaches have been introduced and are gradually implemented [5].

Human periodontal ligament-derived mesenchymal stromal cells (hPDLMSCs), which originate from neural crest cells (NCCs) at the embryogenetic stage, have been identified as possessing stem cell-like properties capable of generating cells related to periodontal tissue [6]. Animal studies have also demonstrated the regenerative abilities of hPDLMSCs, forming periodontium-like structures with cementum-like tissue and well-oriented PDL-like fibers in defective sites [7,8]. Consequently, without considering the limitation in its source, hPDLMSCs are ideal and attractive for periodontal regeneration, including their immunomodulatory functions [9]. However, the necessity of tooth extraction and the heterogeneity of hPDLMSCs greatly challenge the adequate and stable obtention of the cells, and significantly limit the clinical application of hPDLMSCs in regenerative therapy [5].

Because of their self-renewal and multipotent properties, coupled with increasingly efficient and safer reprogramming techniques, human induced pluripotent stem cells (hiPSCs) have provided a promising platform for the cure of diverse diseases such as corneal disorder, heart failure and spinal cord injury [10–13]. Therefore, the strategy that utilizing hiPSCs as a robust and applicable supply for hPDLMSCs generation has been on going [14]. Previous studies have indicated that hiPSC-derived neural crest-like cells (NCLCs) can be further induced into hPDL stem cell-like cells (hPDLSC-like cells) by culturing with extracellular matrix (ECM) from hPDLSCs [15]. However, the production of ECM from hPDLSCs still needs the harvesting of primary cells, which cannot fundamentally solve the problem of cell source. Hence, optimal and applicable induction strategies of hPDLMSCs based on the stimulation of growth factors need to be investigated for practical application.

In this study, we evaluated the induction methods of induced NCLCs (iNCLCs) from hiPSCs depending on different ECMs (fibronectin and laminin; FN and LM) and evaluated their mesenchymal differentiation potential for downstream application of generating hPDLMSC-like cells. Based on our method using FN for iNCLCs derivation, we further investigated the differentiation strategy for hPDLMSC-like cells generation by administrating different recombinant growth factors, including fibroblast growth factor 8b (FGF8b), FGF2, bone morphogenetic protein 4 (BMP4) and Ectodysplasin A (EDA), and finally found that FGF2+FGF8b+BMP4 growth factor cocktail was most effective. Our findings contributed to understanding the molecular basis of hPDLMSCs development and demonstrated the potential of hiPSCs for hPDLMSCs generation as an effective and novel applicable approach.

## 2. Materials and methods

### 2.1. Ethics statement

This study was conducted according to the principles expressed in the Declaration of Helsinki. The study was approved by the Institutional Review Board of Tokyo Medical and Dental University Human Subjects Research (D2020-077). All patients or guardians were fully informed and gave written consent for the donation of their teeth and their subsequent use in this research project.

### 2.2. Cell culture

#### 2.2.1. Cell maintenance

hiPSCs 1231A3 were purchased from RIKEN BRC (Tsukuba, Japan), cultured on a vitronectin (Thermo Fisher Scientific, Massachusetts, United States)-coated 6-well cell plate with a density of $1 \times 10^4$ cells per well, and maintained in StemFit AK02N (Ajinomoto, Tokyo, Japan). Cell passaging was conducted once a week. Feeder free cell line 1231A3, was detached with TrypLE select (Thermo Fisher Scientific) supplemented with 0.25 mM EDTA (nacalai tesque, Kyoto, Japan). Colonies were dissociated manually into single cells and then re-seeded in maintenance medium containing 10 μM ROCK inhibitor (Y-27632; FUJIFILM Wako, Tokyo, Japan). The medium was initially changed the following day to remove the ROCK inhibitor, then it was replaced every other day. hPDLMSCs were isolated from healthy patients as previously reported [16], and were cultured in each T-225 flask with a density of $1 \times 10^5$ cells. A basic medium consisting of alpha-minimum essential medium (α-MEM; Thermo Fisher Scientific) supplemented with 10% fetal bovine serum (FBS; Thermo Fisher Scientific), 100 U $ml^{-1}$ penicillin and 100 μg $ml^{-1}$ streptomycin (P/S; Thermo Fisher Scientific), was utilized for hPDLMSCs maintenance, and as a standard for evaluating the differentiation of cells induced from hiPSCs. Weekly cell passaging was followed. Cells were detached with 0.25% Trypsin-EDTA (Thermo Fisher Scientific) and then re-seeded in a new T-225 flask. Medium change was performed every three days for hPDLMSCs. Through all experiments, hiPSCs were used between passage number 18 and 25, while hPDLMSCs were used at passage 7.

#### 2.2.2. NCLCs induction from hiPSCs

Before iNCLCs induction, hiPSCs were detached from vitronectin-coated plates and re-seeded on FN (Sigma-Aldrich, Massachusetts, United States)-coated or LM (iMartrix-511 silk; Nippi, Tokyo, Japan)-coated 12-well plates, with a density of $7.5 \times 10^3$ cells $well^{-1}$ and $2.5 \times 10^3$ cells $well^{-1}$, respectively. Cells were cultured in StemFit AK02N for four days, then stimulated with a differentiation medium consisting of StemFit AK02N without FGF2 (Ajinomoto), 10 μM SB431542 (Sigma-Aldrich) and 1 μM CHIR99021 (FUJIFILM Wako) for 4, 6, 8, 10, or 12 days.

#### 2.2.3. Mesenchymal stem cells induction from hiPSC-derived iNCLCs

As previously reported [17,18], before inducing the MSC, iNCLCs were detached and re-seeded on fibronectin-coated 12-well plates at $1 \times 10^4$ cells/$cm^2$ (Day 0) in iNCLCs maintenance medium consisted of StemFit AK02N without bFGF, supplemented with 10 μM SB431542, 20 ng $ml^{-1}$ epidermal growth factor (EGF; FUJIFILM Wako), and 20 ng $ml^{-1}$ FGF2 (FUJIFILM Wako). After 24 h, the medium was changed to the basic medium (described previously) and cells were cultured for 14 days with every three-day medium change (from Day 1). Cell passaging was performed while cells reached into 80% confluency.

#### 2.2.4. hPDLMSC-like cells induction from hiPSC-derived iNCLCs

Before inducing the hPDLMSCs, iNCLCs were detached, re-seeded, and maintained for 24 h. From Day 1, the culture medium was switched into the basic medium containing 10 ng $ml^{-1}$ FGF2, 100 ng $ml^{-1}$ FGF8b (FUJIFILM Wako), 50 ng $ml^{-1}$ BMP4 (FUJIFILM Wako), 25 ng $ml^{-1}$ EDA (recombinant ectodysplasin A1; R&D Systems, Minnesota, United States). Cells were induced for another 14

days with every other-day medium change and collected for further analysis. Recombinant growth factors were reconstituted according to manufacturers' instructions.

### 2.3. Differentiation assay of induced MSCs (iMSCs)

For evaluating the osteogenic differentiation ability of iMSCs, $5 \times 10^4$ cells were seeded on a 35 mm dish (Falcon, New York, USA) and cultured with osteo-inductive medium consisting of the basic medium containing 82.1 μg $ml^{-1}$ ascorbic acid (FUJIFILM Wako), 10 mM b-*glycero*-phosphate (Sigma-Aldrich), and 10 nM dexamethasone (DEX) (Fuji Pharma, Fuji, Japan) for 21 days. Medium change was performed every three days, and the differentiation properties were evaluated by Alizarin Red staining (FUJIFILM Wako; 1%, PH 5.4, RT) after the brief fixation by 4% paraformaldehyde (Muto Pure Chemicals, Tokyo, Japan) (15 min; 4 °C).

For evaluating the adipogenesis differentiation ability of iMSCs, $5 \times 10^4$ cells were seeded on a 35 mm dish and cultured with adipogenic medium consisting of the basic medium containing 100 nM DEX, 0.5 mM isobutyl-1-methylxanthine (Sigma-Aldrich), and 50 mM indomethacin (FUJIFILM Wako) for 28 days. Medium change was performed every three days, and the differentiation properties were evaluated by Oil Red O staining (FUJIFILM Wako) after the brief fixation by 4% paraformaldehyde (15 min; 4 °C).

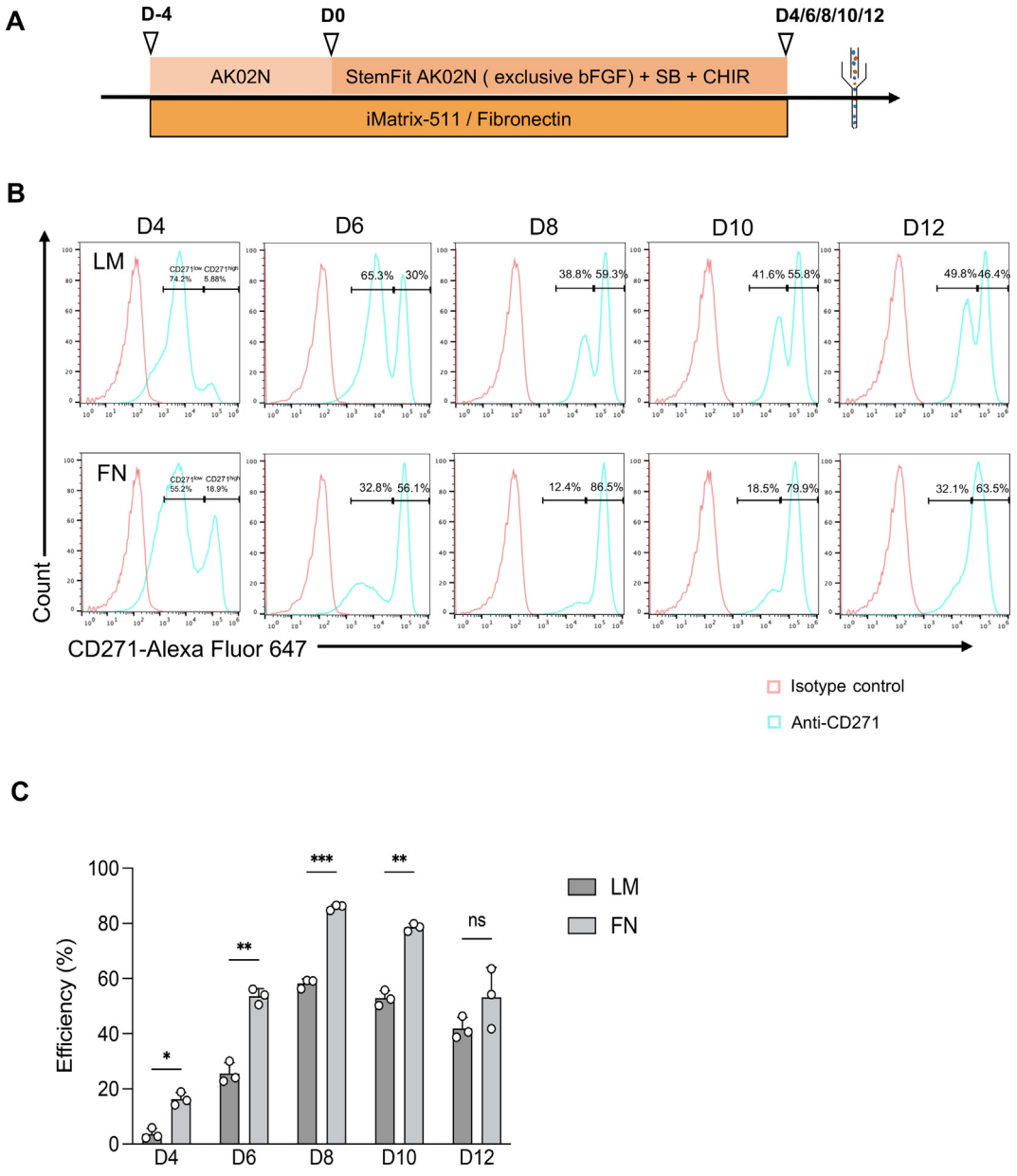


**Fig. 1.** Investigation of the induction strategy of iNCLCs from hiPSCs. **(A)** Schematic diagram of the iNCLCs induction protocol. hiPSCs were cultured in iMatrix-511 (LM)-coated or Fibronectin (FN)-coated condition for 4 days, then the differentiation was induced by SB431542 (SB) and CHIR99021 (CHIR) for 4, 6, 8, 10, or 12 days, respectively, followed by flow cytometry analysis. **(B)** Flow cytometric analysis of CD271 positive cells. Representative histogram plots at each time point were shown, and the percentages of $CD271^{low}$ and $CD271^{high}$ cells in live singlet iNCLCs from different coating methods are annotated (mean of three individual experiments; mean ± SD). **(C)** Bar graph of the percentages of $CD271^{high}$ cells in live singlet iNCLCs from different coating methods. Data are presented as the mean ± SD, n = 3. *P < 0.05, **P < 0.01, ***P < 0.001; by two-way ANNOVA with multiple comparison via Šídák's test.

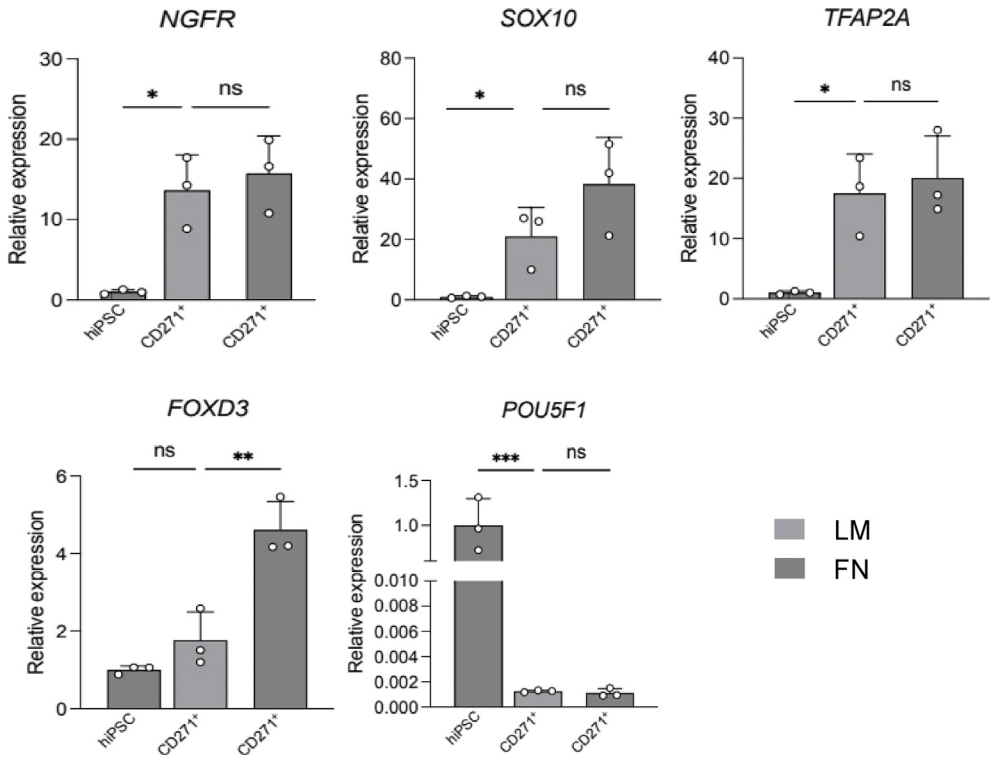


**Fig. 2.** Evaluation of the influence of different coating materials on the gene expression of stem cell-related markers. The relative expression of pluripotency marker gene (*POU5F1*), and NCC-related genes (*NGFR*, *SOX10*, *TFAP2A*, and *FOXD3*) in hiPSCs, sorted CD271$^+$ cells from different coating material conditions. CD271-positive cells were isolated by magnetic-activated cell sorting. hiPSCs = 1; n = 3. Data are presented as the mean ± SD. *P < 0.05, **P < 0.01, ***P < 0.001; by one-way ANOVA with multiple comparison via Dunnett test.

### 2.4. Flow cytometry analysis

Cells were detached from culture plates using TrypLE select with 0.25 mM EDTA according to the manufacturer's instructions. After performing surface staining with fluorescent-conjugated antibodies diluted in staining buffer (2% FBS/DPBS) at 4 °C for 30 min, cells were washed and resuspended in staining buffer. Each sample was dyed by 7-AAD routinely for discrimination of dead cells, then analyzed by Attune NxT (Thermo Fisher Scientific). Data were analyzed with Flowjo Software V10 (BD Bioscience, New Jersey, US).

### 2.5. Magnetic-activated cell sorting

Differentiated cells were sorted by EasySep™ Release Human PSC-Derived Neural Crest Cell Positive Selection Kit (STEMCELL Technologies, Vancouver, Canada) according to the manufacturer's instructions.

### 2.6. RT-qPCR

Total RNA was extracted from hiPSC-derived iNCLCs by RNeasy Mini Kits (Qiagen, Dusseldorf, Germany), according to the protocol manufacturer described. cDNA was synthesized from 300 ng of total RNA using the Superscript VILO cDNA Synthesis Kit (Thermo Fisher Scientific). RT-qPCR was performed with TaqMan Fast Advanced Master Mix (Thermo Fisher Scientific) utilizing the thermal cycler dice real time system ii TP910 (TaKaRa-Bio, Shiga, Japan). The primers were listed in. The relative expression levels normalized to internal reference control (*ACTB*) were calculated by the delta delta Ct method.

### 2.7. Statistical analysis

All data shown in the graphs are presented as mean ± standard error of the mean values from at least three independent experiments. Statistical analyses were performed using Prism 10 (GraphPad software, Boston, US). For comparisons among more than two groups, significance was determined by one-way analysis of variance (ANOVA) with Šídák's multiple comparisons test. For comparisons among grouped data, two-way ANOVA with multiple comparisons Dunnett's test was used. $P < 0.05$ was considered statistically significant ($^{*}P < 0.05$; $^{**}P < 0.01$; $^{***}P < 0.001$; $^{****}P < 0.0001$; ns, $P > 0.05$).

## 3. Results

### 3.1. Modifying the efficiency of CD271$^{high}$ cells induction by FN-coating method

Since the previous study showed that CD271$^{high}$ NCLCs were applicable for MSC induction, we tried to induce them from the feeder-free hiPS cell line 1231A3 as the cell source for hPDLMSCs generation (Fig. 1A). However, the induction efficiency of NCLCs confirmed by flow cytometry indicated that it was insufficient when using LM coating as suggested by previous research (Fig. 1B). To solve this problem, we attempted to induce the differentiation via FN coating because it was used as ECM in

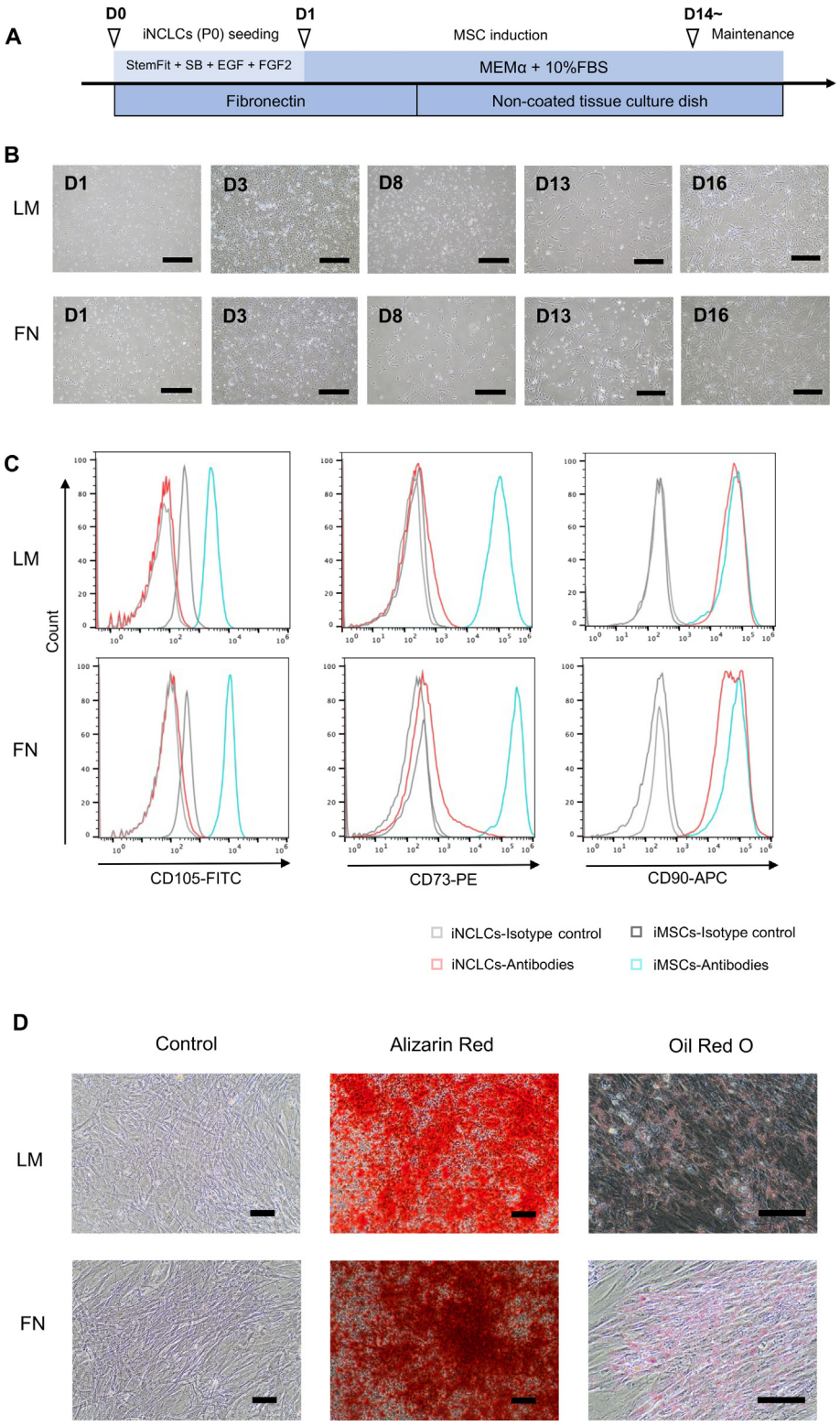


**Fig. 3.** Verification of mesenchymal potential of NCLCs induced from different coating materials. (A) Schematic diagram of the iMSCs induction protocol. iNCLCs induced from LM/FN-coated condition were maintained in StemFit AK02N medium (exclusive bFGF) with EGF and FGF2, SB for 24 h. MSC differentiation was stimulated by basic complete medium for 14 days, Flowcytometric analysis were performed on day14. (B) Representative images of cells at different time points of iMSCs induction. Scale bar = 500 μm. (C) Flow cytometric analysis of MSC-related surface markers (CD34, CD90, and CD105) in LM/FN-iNCLCs and LM/FN-iMSCs. Representative histogram plots are shown. (D) Evaluation of multipotent differentiation properties of LM/FN-iMSCs from LM/FN condition. Representative images of alizarin red staining (for osteogenesis) and oil red O staining (for adipogenesis) are shown. Scale bar = 100 μm.

the NCLCs maintenance. Surprisingly, the induction efficiency peaked on day 8 among the methods, and the percentages of CD271$^{high}$ cells were significantly higher in the FN group than the LM group (Fig. 1B and C), suggesting the better NCLC induction potential of FN.

### 3.2. Characterization of iNCLCs induced by two different coating methods

Considering the possibility that differentiation methods might affect the characteristics of the induced cells, we tested the expression of NCC-related genes as a criterion. Comparable in two methods, *POU5F1*, a pluripotent stem cell marker, showed a similar reduction in all induced cells, suggesting that the coating material did not interfere with the differentiation process of hiPSCs (Fig. 2). Meanwhile, sorted CD271$^{+}$ cells from both conditions demonstrated higher expression of NCC-related genes (*NGFR*, *SOX10*, and *TFAP2A*) than hiPSCs, indicating that the pluripotent stem cells were induced towards the direction of neural crest, and the characteristics of sorted CD271$^{+}$ cells were similar between the methods (Fig. 2). Notably, *FOXD3,* one of the first markers for NCCs specification during their development, was expressed at higher levels in captured FN-induced CD271$^{+}$ cells than in LM-induced cells. This result was consistent with flow cytometric analysis (Fig. 1B), indicating the better induction efficiency of the CD271$^{high}$ population in the FN-coated condition.

Next, due to our main objective and the need to verify the availability of our iNCLC generation method, we tested the mesenchymal potential of LM/FN-induced iNCLCs (LM/FN-iNCLCs) by culturing the cells of passage 0 in MSC-inductive media for 14 days (Fig. 3A). The morphology of the cells after reseeding showed the original neural crest-like shape of active multipolar with narrow projections, then began to change slimmer and longer from day 3. With the progression of differentiation, it was found that the induced cells tended to close to MSC-like morphology, which was characterized as elongated, fibroblastic-like, spindle-shaped transforming forms (Fig. 3B). After inducing MSC differentiation for 14 days, we examined three commonly known MSC-related surface markers (CD73, CD105, and CD90) in iMSCs. CD105 and CD73 were negative in undifferentiated LM/FN-iNCLCs but highly expressed in iMSCs, while CD90 was highly expressed in both populations (Fig. 3C). Additionally, the markers representative of immune cells (CD45, CD34, CD11b, CD19, and HLA-DR) were simultaneously negative in iMSCs (Appendix Fig. 2), proving that the direction of differentiation was toward the MSCs side. Based on the fact that the expression pattern of MSC-related markers of iMSCs induced from LM/FN-iNCLCs was normal, we verified their osteogenic and adipogenic differentiation potency *in vitro* by alizarin red and oil red O staining, respectively (Fig. 3D). At the same time, osteogenesis-related genes (*SPP1* and *BGLAP*) and adipogenesis-related genes (*LPL* and *PPARγ*) were confirmed in corresponding samples as well (Appendix Fig. 3). Considering that the mesenchymal multipotent characteristics of iMSCs induced from FN-iNCLCs were similar to those of iNCLCs derived from LM condition (Fig. 3D), the FN-coating method demonstrated better efficiency in inducing iNCLCs that ideal for producing the iMSCs in our experiment.

### 3.3. hPDLMSC-like cells generation from iNCLCs

For hPDLMSC-like cells generation, we focused on FGF8b, well known as a trigger signal coming from epithelium [19], as the main growth factor and examined the effects of FGF8b with other vital cytokines during development. Built on our robust protocol of NCLCs generation, we treated FN-iNCLCs of passage 0 in MSC-inductive media with FGF8b and FGF2 as basal, and added BMP4 (BMP4+ group), EDA (EDA+ group) or both of them (BMP4/EDA+ group) for 14 days (Fig. 4A). Setting iMSCs as a control, the mRNA expression levels of typical dental mesenchyme-related genes (*PAX9* and *LHX8*, highly expressed in hPDLMSCs as well [20]) were significantly upregulated in BMP4+ or BMP4/EDA+ group rather than EDA+ group. Meanwhile, *DLX1* expression was relatively consistent between treated groups but upregulated when compared with iMSCs. *MSX1* expression was lower than iNCLCs and had no clear change in each experimental group (Fig. 4B and Appendix Fig. 4B). In addition, *FOXF1* and *FOXF2*, the dental follicle markers [21,22] and high-expressing genes in hPDLMSCs [20], were also analyzed. Notably, their expressions were significantly upregulated compared to iMSCs, especially in the BMP4+ group. Besides, we also examined the temporal effects of BMP4 and EDA stimulation on different stages of differentiation (specific groups were described as cytokine + addition period, such as BMP4+D1-7 for cells added BMP4 during day 1 to day 7; Appendix Fig. 4A). We found that *PAX9* and *LHX8* were mainly upregulated in BMP4+D1-7 and D8-14 or BMP4/EDA+ D1-7 and D8-14 groups, which clearly indicated that the addition of BMP4 at an earlier stage was better for their differentiation initiation. But for *FOXF2*, its expression was mainly enhanced in the BMP4+D8-14 or BMP4+D1-14 group, suggesting that BMP4 would have a major effect on *FOXF2* expression at a later stage. These results illustrated the possibility that growth factor-mediated stimulatory signal has a temporal sequentiality associated with different stages of hPDLMSCs development, which may be related to the activation of different transcription factors (TFs) (Appendix Fig. 4B).

Furthermore, we confirmed the expression levels of *S100A4* and *POSTN*, the markers that reported relatively expressing higher in human periodontal ligament (hPDL) cells compared to bone marrow mesenchymal stem cells (BMMSCs) or human gingival fibroblasts (hGFs) [16]. *POSTN* was upregulated in the BMP4+D1-14 group when compared to hPDLMSCs, but highly expressed in iMSCs at the same time (Fig. 5 and Appendix Fig. 5). There was no significant difference in *S100A4* gene expression between treatment groups, but it displayed higher compared with iNCLCs and iMSCs. Together, these results suggest that BMP4 can effectively promote the differentiation of neural crest mesenchyme into hPDLMSC-like cells under the stimulation of FGF8b and FGF2.

## 4. Discussion

Aiming to induce hPDLMSC-like cells from hiPSCs, NCC induction is an indispensable step from the perspective of embryonic development. At the beginning of our project, we followed the previously reported protocol to generate iNCLCs [18]. However, we failed to achieve enough efficiency with the original protocol due to the possible nuances in inductive media components, the maintenance period, the condition of hiPSCs or the lot of coating materials. Therefore, we discussed different conditions (coating materials and inductive periods) during the generation process of iNCLCs. Based on the previous research [23], FN is a better ECM for NCCs maintenance and growth than LM, but few studies have applied it for iNCLCs induction from hiPSCs before. A comparison between two coating materials in our study interestingly showed that cells exhibited a “2D-3D-2D” hybrid culture phenomenon in FN-coated culture condition (Appendix Fig. 1), which was partially similar to the process of NCCs induction from embryonic stem cells (ESCs) by the way of embryonic body (EB) formation [23]. We speculated that this phenomenon was mainly due to the difference in adhesion ability of hiPSCs between materials. According to the study focusing on different coating methods in hiPSCs culture, FN was the only material with lower electrical potential as an uncoated surface [24].

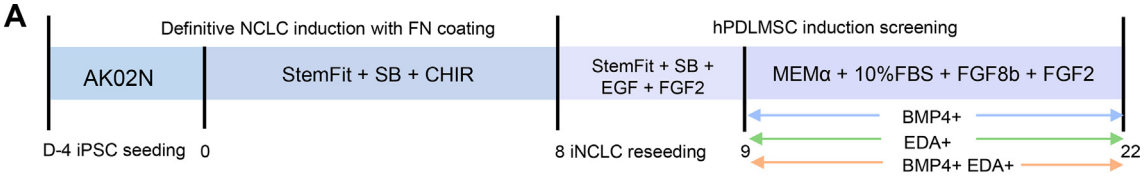
A
Definitive NCLC induction with FN coating
hPDLMSC induction screening
AK02N
StemFit + SB + CHIR
StemFit + SB + EGF + FGF2
MEMα + 10%FBS + FGF8b + FGF2
BMP4+
EDA+
BMP4+ EDA+
D-4 iPSC seeding
0
8 iNCLC reseeding
9
22

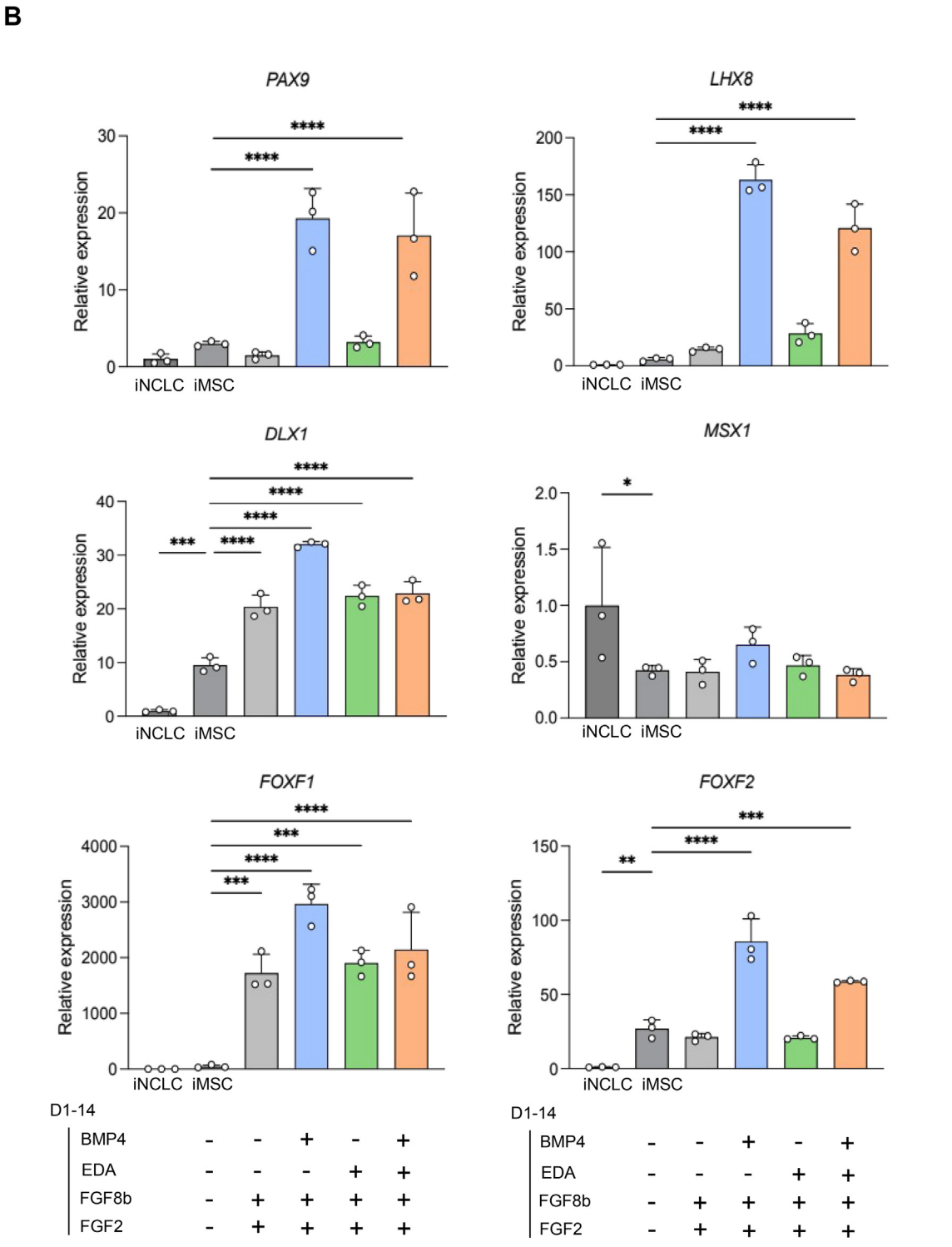
B
PAX9
LHX8
DLX1
MSX1
FOXF1
FOXF2
Relative expression
iNCLC
iMSC
D1-14
BMP4
EDA
FGF8b
FGF2

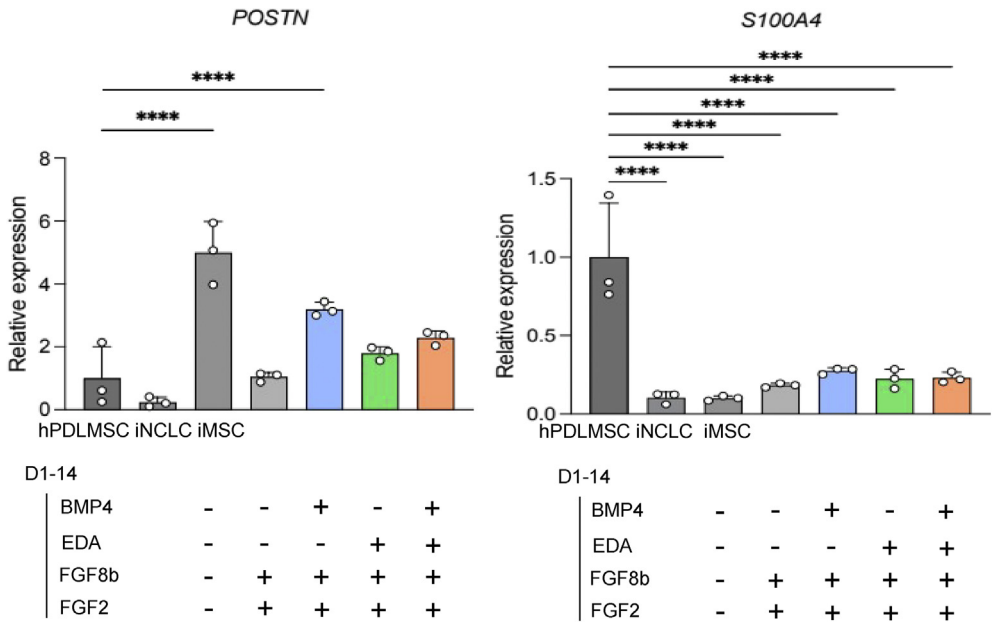


**Fig. 5.** Evaluation of hPDL-related genes in induced hPDLMSC-like cells. The relative expression of hPDL-related genes (*POSTN* and *S100A4*) in hPDLMSCs, iNCLCs, iMSCs and induced hPDLMSC-like cells with the stimulation of growth factors for 14 days. hPDLMSCs = 1; n = 3. Data are presented as the mean ± SD. *P < 0.05, **P < 0.01, ***P < 0.001, ****P < 0.0001, ns. is not shown; by one-way ANOVA with multiple comparison via Dunnett test. (compared to hPDLMSCs).

Considering that the cell surface usually has a negative resting potential [25], this factor may have provided an inadequate adhesive environment for hiPSCs and led to the formation of a 3D structure in the early period like suspension culture [23]. Nevertheless, as the iNCLCs induction progressed, cells migrated out of the EB-like structures and reattached to plates for NCC differentiation like LM-coated samples (Appendix Fig. 1). In addition, these FN-iNCLCs had a higher differentiation efficiency while maintaining similar characteristics to LM-coated induced cells, with the similar ability of iMSCs induction as well (Figs. 1–3). Although the specific mechanism of the phenomenon deserves further investigation, our FN-coating induction method realized better production efficiency for iNCLCs that did not need further purifications.

In the phenotypic evaluation of iNCLCs, we found that NCC-related markers were enriched in sorted $CD271^+$ cells. Notably, the gene expression of *FOXD3* and *SOX10* was higher in the FN-$CD271^+$ cell population than in the LM-$CD271^+$ cell population. *FOXD3* and *SOX10* are well-known as vital TFs that are activated in response to the BMP and WNT signalings, which are important for the NCCs identification [26]. Meanwhile, their functions in NCC specification, multipotency maintenance and migration also indicated their essential roles during the differentiation [27]. While these findings partially explained the higher efficiency of iNCLC induction, the relationship between the FN coating condition and the expression of *FOXD3* and *SOX10* remains to be elucidated. Considering that previous study showed that fibronectin is the only substrate tested that can promote the migration of NCC *in vitro* [28], the difference in *FOXD3* and *SOX10* expression between coating materials may be related to the migratory ability of iNCLCs in FN.

Researchers have been studying the specific markers of hPDLMSCs for a long time, but they are not yet available. According to the previous studies, hPDLMSCs displayed the high expression on typical dental mesenchyme-related genes such as *MSX1* and *LHX8*, as well as the DF-related marker *FOXF1*. These characteristics distinguished hPDLMSCs from MSCs of other various origins and extra somatic stem cells [20]. Noticeably, *LHX8* exhibited higher expression levels than MSCs derived from jaw bones, same origin as hPDLMSCs, making it available as specific marker for hPDLMSCs examination. Aside from that, *PAX9* and *FOXF2* were also found to be highly expressed in hPDLSCs and *PAX9* was identified as responsible factor for hPDLSCs induction [29], which can be a candidate to discriminate the feature of hPDLMSCs as well.

It has been reported that the odontogenic capacity of mouse dental mesenchyme (DM) would disappear when cultured *in vitro* without dental epithelium (DE) [30], suggesting that the oral ectoderm signalings played an important role in DM development [31,32]. FGF8b has been reported to be a key odontogenic factor, and it functions on the expression of a specific group of TFs represented by *DLX*, *PAX9*, *LHX8*, and *MSX1*, which have been well demonstrated to be expressed in DM [33,34]. Meanwhile, since FGF2 played a positive role in cell expansion during the induction process [35,36], we set FGF8b and FGF2 as basic cytokines for the induction of hPDLMSC-like cells from iNCLCs. With the combination of BMP4 or EDA, it is shown that BMP4 + FGF8b + FGF2 induced higher expression of DM-related markers (*PAX9*, *LHX8*, and *DLX1*), DF-related (*FOXF1* and *FOXF2*) and hPDL-related genes (*POSTN* and *S100A4*) compared with iNCLCs (Fig. 4), which represented the process of transition into hPDLMSC-like cells from neural-crest-like mesenchyme. Comparatively, *MSX1* expression

**Fig. 4.** hPDLMSC-like cells induction from hiPSC-derived iNCLCs. (A) Schematic diagram of the hPDLMSC induction screening. Through definitive NCLC induction protocol, iNCLCs induced from FN-coated condition were maintained in StemFit AK02N medium (exclusive bFGF) with EGF and FGF2, SB for 24 h. hPDLMSC differentiation was stimulated by basic complete medium with FGF8b and FGF2 for 14 days, BMP4/EDA-adding was screened by qPCR. (B) The relative expression of dental mesenchyme-related genes (*PAX9*, *LHX8*, *DLX1*, and *MSX1*), and dental follicle-related genes (*FOXF1* and *FOXF2*) in iNCLCs, iNCLCs-derived iMSCs, and induced hPDLMSC-like cells with the stimulation of growth factors for 14 days. iNCLC = 1; n = 3. Data are presented as the mean ± SD. *P < 0.05, **P < 0.01, ***P < 0.001, ****P < 0.0001, ns. is not shown; by one-way ANOVA with multiple comparison via Dunnett test (compared to iMSCs).

was reduced by FGF8b + FGF2 stimulation and rescued to some extent by the application of BMP4, which is consistent with previous studies reporting that BMP4 is essential for the activation of *MSX1* expression in DM development [37,38]. Although EDA has been suggested to play an active role in tooth initiation and tooth root development [32], it did not appear to have an obvious effect on hPDLMSCs induction in our experiment. The functions and the action sequence of these TFs should be further analyzed to refine the complicated and multi-organized process of hPDLMSCs development.

Furthermore, the stream of NCCs fated into dental mesenchyme should be coming from the first branchial arch (BA1), and the hPDLMSC-like cells should also be generated from iNCLCs with the characteristic of specific NCCs related to BA1. However, it is still difficult to determine specific makers of NCCs from BA1, and the TGF-beta inhibition/WNT activation protocol tended to derive heterogeneous NCC populations [18]. These facts also lead to insufficiency of refined control of hPDLMSC-like cells induction and make hPDLMSC-like cells partially different from the original hPDLMSCs yet (Fig. 4). Although our study succeeded in generating hPDLMSC-like cells expressing part of hPDL cells makers using FGF8b, FGF2, and BMP4, we still lack the investigation of other signaling pathways related to tooth formation. For example, WNT and SHH, which have been reported to have interactive crosstalk with FGF, BMP, and EDA signaling pathways [39–42], are valuable for additional assessment for further optimization of hPDLMSCs induction. Besides, the functional properties especially the vivo evaluation of hPDLMSC-like cells also need to be analyzed in the next step.

## 5. Conclusion

With the unexpected finding of the prominent effect of FN coating in the iNCLCs derivation, we demonstrated the importance of ECM in NCCs induction. Moreover, our FGF8b + FGF2 + BMP4 strategy preliminary established the basis for hPDLMSC-like cell induction from iNCLCs. Although investigations for multiple signaling relationships and optimizations for differentiation strategy are still needed, our work has taken the application of hiPSCs for hPDLMSCs generation to the next level.

## Declaration of conflicting interests

The authors declared no potential conflicts of interest with respect to the research, authorship, and/or publication of this article.

## Acknowledgement

We would like to extend our heartfelt gratitude to Dr. Anhao Liu, from Tokyo Medical and Dental University, for his invaluable support and guidance on the critical revision of the manuscript throughout this research. Human iPS cell line 1231A3 was provided by the RIKEN BRC through the National Bio-Resource Project of the MEXT/AMED, Japan.

## Appendix A. Supplementary data

Supplementary data to this article can be found online at https://doi.org/10.1016/j.reth.2024.05.005.

## References

[1] Kinane DF, Stathopoulou PG, Papapanou PN. Periodontal diseases. Nat Rev Dis Prim 2017;3(1):17038.
[2] WHO. Oral health 14 March. World Health Orgnization; 2023. https://www.who.int/news-room/fact-sheets/detail/oral-health.
[3] Liang Y, Luan X, Liu X. Recent advances in periodontal regeneration: a biomaterial perspective. Bioact Mater 2020;5(2):297–308.
[4] Onizuka S, Iwata T. Application of periodontal ligament-derived multipotent mesenchymal stromal cell sheets for periodontal regeneration. Int J Mol Sci 2019;20(11).
[5] Nuñez J, Vignoletti F, Caffesse RG, Sanz M. Cellular therapy in periodontal regeneration. Periodontology 2000;79(1):107–16. 2019.
[6] Seo BM, Miura M, Gronthos S, Bartold PM, Batouli S, Brahim J, et al. Investigation of multipotent postnatal stem cells from human periodontal ligament. Lancet 2004;364(9429):149–55.
[7] Lei M, Li K, Li B, Gao LN, Chen FM, Jin Y. Mesenchymal stem cell characteristics of dental pulp and periodontal ligament stem cells after in vivo transplantation. Biomaterials 2014;35(24):6332–43.
[8] Tsumanuma Y, Iwata T, Kinoshita A, Washio K, Yoshida T, Yamada A, et al. Allogeneic transplantation of periodontal ligament-derived multipotent mesenchymal stromal cell sheets in canine critical-size supra-alveolar periodontal defect model. Biores Open Access 2016;5(1):22–36.
[9] Tomokiyo A, Yoshida S, Hamano S, Hasegawa D, Sugii H, Maeda H, et al. Detection, characterization, and clinical application of mesenchymal stem cells in periodontal ligament tissue. Stem Cell Int 2018;2018:5450768.
[10] Yamanaka S. Pluripotent stem cell-based cell therapy-promise and challenges. Cell Stem Cell 2020;27(4):523–31.
[11] Hayashi R, Ishikawa Y, Sasamoto Y, Katori R, Nomura N, Ichikawa T, et al. Co-ordinated ocular development from human iPS cells and recovery of corneal function. Nature 2016;531(7594):376–80.
[12] Nakamura M, Okano H. Cell transplantation therapies for spinal cord injury focusing on induced pluripotent stem cells. Cell Res 2013;23(1):70–80.
[13] Morita K, Nakamura A, Machida M, Kawasaki T, Nakanishi R, Ichida J, et al. Efficient reprogramming of human fibroblasts using RNA reprogramming with DAPT and iDOT1L under normoxia conditions. Regenerative Therapy 2022;21:389–97.
[14] Hu L, Liu Y, Wang S. Stem cell-based tooth and periodontal regeneration. Oral Dis 2018;24(5):696–705.
[15] Extracellular matrix from periodontal ligament cells could induce the differentiation of induced pluripotent stem cells to periodontal ligament stem cell-like cells. Stem Cell Dev 2018;27(2):100–11.
[16] Iwata T, Yamato M, Zhang Z, Mukobata S, Washio K, Ando T, et al. Validation of human periodontal ligament-derived cells as a reliable source for cytotherapeutic use. J Clin Periodontol 2010;37(12):1088–99.
[17] Fukuta M, Nakai Y, Kirino K, Nakagawa M, Sekiguchi K, Nagata S, et al. Derivation of mesenchymal stromal cells from pluripotent stem cells through a neural crest lineage using small molecule compounds with defined media. PLoS One 2014;9(12):e112291.
[18] Kamiya D, Takenaka-Ninagawa N, Motoike S, Kajiya M, Akaboshi T, Zhao C, et al. Induction of functional xeno-free MSCs from human iPSCs via a neural crest cell lineage. NPJ Regenerat Med 2022;7(1):47.
[19] Prochazka J, Prochazkova M, Du W, Spoutil F, Tureckova J, Hoch R, et al. Migration of founder epithelial cells drives proper molar tooth positioning and morphogenesis. Dev Cell 2015;35(6):713–24.
[20] Onizuka S, Yamazaki Y, Park SJ, Sugimoto T, Sone Y, Sjöqvist S, et al. RNA-sequencing reveals positional memory of multipotent mesenchymal stromal cells from oral and maxillofacial tissue transcriptomes. BMC Genom 2020;21(1):417.
[21] Jing J, Feng J, Yuan Y, Guo T, Lei J, Pei F, et al. Spatiotemporal single-cell regulatory atlas reveals neural crest lineage diversification and cellular function during tooth morphogenesis. Nat Commun 2022;13(1):4803.
[22] Aitola M, Carlsson P, Mahlapuu M, Enerbäck S, Pelto-Huikko M. Forkhead transcription factor FoxF2 is expressed in mesodermal tissues involved in epithelio-mesenchymal interactions. Dev Dynam 2000;218(1):136–49.
[23] Bajpai R, Chen DA, Rada-Iglesias A, Zhang J, Xiong Y, Helms J, et al. CHD7 cooperates with PBAF to control multipotent neural crest formation. Nature 2010;463(7283):958–62.
[24] Tian Z, Wang CK, Lin FL, Liu Q, Wang T, Sung TC, et al. Effect of extracellular matrix proteins on the differentiation of human pluripotent stem cells into mesenchymal stem cells. J Mater Chem B 2022;10(30):5723–32.
[25] Metwally S, Stachewicz U. Surface potential and charges impact on cell responses on biomaterials interfaces for medical applications. Mater Sci Eng C 2019;104:109883.
[26] Simões-Costa MS, McKeown SJ, Tan-Cabugao J, Sauka-Spengler T, Bronner ME. Dynamic and differential regulation of stem cell factor FoxD3 in the neural crest is Encrypted in the genome. PLoS Genet 2012;8(12):e1003142.
[27] Lai X, Liu J, Zou Z, Wang Y, Wang Y, Liu X, et al. SOX10 ablation severely impairs the generation of postmigratory neural crest from human pluripotent stem cells. Cell Death Dis 2021;12(9):814.
[28] Lai X, Liu J, Zou Z, Wang Y, Wang Y, Liu X, et al. Integrin α5β1 supports the migration of Xenopus cranial neural crest on fibronectin. Dev Biol 2003;260(2):449–64.
[29] Sugiura R, Hamano S, Tomokiyo A, Hasegawa D, Yoshida S, Sugii H, et al. PAX9 is involved in periodontal ligament stem cell-like differentiation of human-induced pluripotent stem cells by regulating extracellular matrix. Biomedicines 2022;10(10).
[30] Zheng Y, Jia L, Liu P, Yang D, Hu W, Chen S, et al. Insight into the maintenance of odontogenic potential in mouse dental mesenchymal cells based on transcriptomic analysis. PeerJ 2016;4:e1684.

[31] Thesleff I, Sharpe P. Signalling networks regulating dental development. Mech Dev 1997;67(2):111–23.
[32] Fons Romero JM, Star H, Lav R, Watkins S, Harrison M, Hovorakova M, et al. The impact of the Eda pathway on tooth root development. J Dent Res 2017;96(11):1290–7.
[33] Trumpp A, Depew MJ, Rubenstein JL, Bishop JM, Martin GR. Cre-mediated gene inactivation demonstrates that FGF8 is required for cell survival and patterning of the first branchial arch. Genes Dev 1999;13(23):3136–48.
[34] Zhou C, Yang G, Chen M, He L, Xiang L, Ricupero C, et al. Lhx6 and Lhx8: cell fate regulators and beyond. Faseb J 2015;29(10):4083–91.
[35] Dupuis V, Oltra E. Methods to produce induced pluripotent stem cell-derived mesenchymal stem cells: mesenchymal stem cells from induced pluripotent stem cells. World J Stem Cell 2021;13(8):1094–111.
[36] Xu J, Lian W, Chen J, Li W, Li L, Huang Z. Chemical-defined medium supporting the expansion of human mesenchymal stem cells. Stem Cell Res Ther 2020;11(1):125.
[37] Tucker AS, Al Khamis A, Sharpe PT. Interactions between Bmp-4 and Msx-1 act to restrict gene expression to odontogenic mesenchyme. Dev Dynam 1998;212(4):533–9.
[38] Jia S, Zhou J, Gao Y, Baek JA, Martin JF, Lan Y, et al. Roles of Bmp4 during tooth morphogenesis and sequential tooth formation. Development 2013;140(2):423–32.
[39] Yu M, Wong SW, Han D, Cai T. Genetic analysis: Wnt and other pathways in nonsyndromic tooth agenesis. Oral Dis 2019;25(3):646–51.
[40] Zhang F, Song J, Zhang H, Huang E, Song D, Tollemar V, et al. Wnt and BMP signaling crosstalk in regulating dental stem cells: implications in dental tissue engineering. Genes Dis 2016;3(4):263–76.
[41] O'Connell DJ, Ho JW, Mammoto T, Turbe-Doan A, O'Connell JT, Haseley PS, et al. A Wnt-Bmp Feedback Circuit controls intertissue signaling dynamics in tooth organogenesis. Sci Signal 2012;5(206). ra4-ra4.
[42] Aurrekoetxea M, Irastorza I, García-Gallastegui P, Jiménez-Rojo L, Nakamura T, Yamada Y, et al. Wnt/β-Catenin regulates the activity of epiprofin/Sp6, SHH, FGF, and BMP to coordinate the stages of odontogenesis. Front Cell Dev Biol 2016;4:25.